

Effect of Suction Slot Location and Width on the Performance of Centrifugal Fan

S. A. Beskales^{1,*}, Ibrahim Shahin¹, Samir S. Ayad¹, Osama E. Abdullatif¹ and Tarek A. Mekhail²

¹ Department of Mechanical Engineering, Faculty of Engineering at Shoubra, Benha University, Shoubra, Cairo, Egypt.

² Department of Mechanical Engineering, Faculty of Energy Engineering- Aswan University, Aswan, Egypt.

*Corresponding author

E-mail address: samer.aagaiby@feng.bu.edu.eg, ibrahim.shahin@feng.bu.edu.eg, samir_ayad@mail.com, osama.abdellatif@feng.bu.edu.eg, mina_tarek@hotmail.com

Abstract: Blade slots are known to reduce the noise and improve flow behavior and steadiness in centrifugal fans. The present work considers an unsteady Computational Fluid Dynamic (CFD) study to investigate the effectiveness of slot location and width on the performance and flow field inside the centrifugal fan blade passages. The computer program, Fluent 19, is used and the 3D fan model is validated by comparing its results with those of earlier researchers. The aim of the present study is to find the best slot location and appropriate slot width at that location. The flow pattern is then analyzed and simulated with no slot and with a slot at six different radial locations; namely S1, S2, S3, S4, S5, and S6 with fixed slot width W of 2.5 mm. The computationally generated characteristics of unsteady flow demonstrated that although cut slots at all locations on the fan blade from the hub to the shroud has a negative influence on the centrifugal fan efficiency as well as the static pressure rise compared with the fan without slot, the slots added at S3 i.e. near the midpoint of the blade span gives the highest fan efficiency and largest increase in static pressure. Slots at S3 suppress secondary flow at the blade passages and push it to the blade tip. Additionally, streamlines and velocity distributions in impeller passages and over the blade surfaces (pressure and suction sides) validated the slots' benefits. Computations with different slot width; namely 1.5 mm, 3.5 mm, and 5 mm are carried out to find the best slot location and width at the best slot location S3. At the optimal efficiency point, the calculated performance of the employed fan with slot location S3 and 2.5 mm width, showed a 2.7 % increase of efficiency and 1.5% increase in static pressure rise as compared to fans with slot at S1 with same width of 2.5 mm. However, it showed a positive impact on the boundary layer buildup and flow separation over the blade suction side for the impeller studied.

Keywords: Suction Slots, Secondary flow, Centrifugal Fan Performance, CFD, Simulation.

NOMENCLATURE

Symbols	Description	SI units	Symbols	Description
u'	Fluctuated velocity	m/s	Abbreviations	
\overline{U}_i	Time averaged velocity	m/s	BEP	Best Efficiency Point
C_m	Moment Coefficient	-	CFD	Computational Fluid Dynamics
D_s	Slot pitch Diameter	mm	MRF	Moving Reference Frame
k	Turbulent kinetic energy	m^2/s^2	SST	Shear Stress Transport
Greek			SIMPLE	Semi-Implicit Method for Pressure Linked Equations
ρ'	Instantaneous value of density	kg/m^3		
ε	Turbulent energy dissipation rate	m^2/s^3		
ω	Rotational Speed	s^{-1}		
ϕ	Flow coefficient = $Q/\omega D^3$	-		
η	Static Efficiency	-		
ψ	pressure coefficient = $\Delta P/\rho\omega^2 D^2$	-		

1. Introduction

In centrifugal fans, the recirculation zones occurring between the blade passages contribute to some losses. The moving fluid with low velocity in the boundary layer does not remain in the thin layer which sticks to the impeller's blade surfaces. The boundary layer will increase its thickness substantially within the downstream path near

the blade tip and the fluid particles in the boundary layer experience a negative velocity and the flow may be reversed. At the point of the separation one streamline intersects the wall at a definite angle as shown in Fig. 1, and the point of separation itself is determined by the condition that the velocity gradient normal to the blade surface vanishes there.

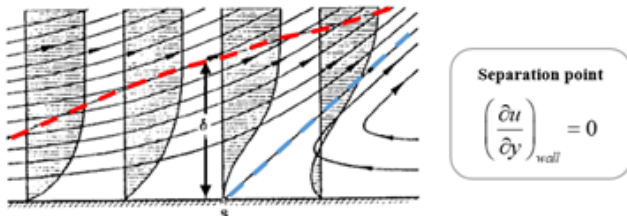


Fig 1. Flow in boundary layer near separation [1]

This study's objective is to enhance the flow on the suction side of the blade's impeller by decreasing the size of the recirculation zones. This can be done by cutting slot in the blades of the impeller to control the flow passively in order to delay flow separations. slot will move the flow from the pressure side of the blade to the suction side, they are installed near the point of separation to control the development of the boundary layer over the blade surface. Many researchers have utilized CFD to investigate centrifugal fan performance. [2] studied numerically the effect of the operating condition, such as the impeller speed, on the centrifugal fan performance and flow characteristics. [3] analyzed both transient simulations and steady moving reference frame (MRF) simulations. [4] studied the effect of blade angles on the velocity and pressure distribution inside the impeller passages using the CFD techniques. Furthermore, detailed information on the flow field through the fan may be collected, providing guidance for fan impeller modification by cutting slots in the impeller blades. [5] investigated the effect of a cut slot in the blower blades, the results showed The magnitude of pressure variations decreases when slots are added to the impeller blades and the fluid poured through the slots into the impeller passages re-energizes the separated flow. [6] Studied the effect of constant-diameter slots in a perpendicular direction to the blade surface on radial fan impeller. The results revealed that the slots enhanced the internal efficiency and overall pressure of the fan impeller without volute casing. [7] analyzed unsteady numerical simulations the slot cuts near the impeller shroud and the results showed that both the performance and flow field are well improved by applying the blade surface slots with 3.6 % for the total pressure and of 2.6 % for the efficiency at the design mass flow rate. Single and twin slot configuration were investigated by [8] at different locations on the chord length from the blade root. The results showed that the optimum single slot size is 5 mm with 5.5 % increase in the static pressure while the twin slot located at 50% and 75% from the blade root with 3 mm slot size enhance the static pressure by 7% compared with the base blade model. [9] studied the effect of the slot on an airfoil, results confirmed the slot benefits in reducing the boundary layer separation and stall control over different incident angles. [10] used a passive control using an opening in the airfoil through which the flow passed and converted the separation region into small vortices. [11] used a slotted blade on a centrifugal pump, which improved hydraulic performance.

2. COMPUTATIONAL TECHNIQUE

2.1 Governing Equations

Researchers utilize CFD to collect information on fluid flow issues and flow parameters such as pressure, velocity in situations when experimental procedures cannot be conducted. This can be achieved by solving the fundamental equations such as conservation of mass and momentum for incompressible turbulent flow [1]

$$\frac{\partial \bar{\rho}}{\partial t} + \frac{\partial}{\partial x_i} [\bar{\rho} \cdot \bar{U}_i] = 0 \quad (1)$$

$$\rho \left(\frac{\partial \bar{U}_i}{\partial t} + \bar{U}_j \frac{\partial \bar{U}_i}{\partial x_j} \right) = -\frac{\partial \bar{P}}{\partial x_i} + \frac{\partial}{\partial x_j} \left(\mu \frac{\partial \bar{U}_i}{\partial x_j} - (\rho \overline{u'_j u'_i}) \right) + \bar{F}_i \quad (2)$$

2.2 Shear Stress Transport (SST) K- ω Model

In the present study, the Shear Stress Transport (SST) k- ω model is implemented. The k- ω model consists of two equations. The Wilcox k- ω model [12] is more stable than the k- ϵ model in the viscous sublayer close to the wall and is one of the most well-known forms of k- ω . However, its results are particularly sensitive to the free stream value of ω in the free shear layer and adverse pressure gradient boundary layer flows. Consequently, the k- ϵ model is not the most appropriate model for wake area applications. In the wake areas, however, the k- ϵ model performs better, according to Menter [13], the combination of the two models is the optimum way to model the flow characteristics along the wall and in the boundary layer's wake. Accordingly, the SST k- ω turbulence is believed to be the best acceptable model for predicting the flow characteristics. The first equation in the model defines the turbulent kinetic energy (k), while the second describes the turbulent dissipation rate (ω).

$$\frac{\partial \rho k}{\partial t} + \frac{\partial \rho k U_j}{\partial x_j} = \frac{\partial}{\partial x_j} \left[(\mu + \sigma_k \mu_t) \frac{\partial k}{\partial x_j} \right] + P_k - \beta^* \rho \omega \quad (3)$$

$$\frac{\partial \rho \omega}{\partial t} + \frac{\partial \rho U_j \omega}{\partial x_j} = \frac{\partial}{\partial x_j} \left[(\mu + \sigma_\omega \mu_t) \frac{\partial \omega}{\partial x_j} \right] + \gamma P \omega - \beta \rho \omega^2 + 2(1 - F_1) \rho \sigma_\omega 2 \frac{\mu_t}{k} \frac{\partial k}{\partial x_j} \frac{\partial \omega}{\partial x_j} \quad (4)$$

3. CFD PROGRAM VALIDATION

3.1 Geometric Model

The aim of this section is to verify the reliability of the CFD model such that it can be used with confidence for numerical simulation and decision making in the design and the modification of centrifugal impeller blades with different slot locations and widths. The predictions of the utilized computer software, FLUENT 19, are validated and compared to the results produced by Schönwald et al. [14] using HP workstation (Intel Xeon E5-2680 V3 -2.5 GHz and 128 GRAM). The modeled centrifugal fan in the present validation is with ten backward impeller blades. The whole fan's design specifications and settings are provided in Table 1 and Fig. 2.

TABLE 1 The design parameters for the centrifugal fan.[14]

Item	Dimension
Angle of cover plate	11 °
Blade inlet angle	31 °
Blade outlet angle	41 °
Curvature of the cover plate	45 mm
Curvature of the inlet nozzle	45 mm
Clearance	3 mm
Clearance width	13 mm
Casing width	315 mm
Curvature of the blade	383 mm
Blade number	10
Diameter of the inlet duct	400 mm
Diameter of impeller outlet	722 mm
Diameter of impeller inlet	318 mm
Blade inlet width	33 mm
Blade outlet width	93 mm

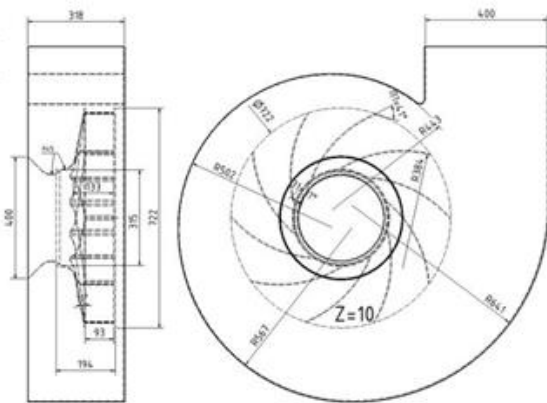


Fig 2. Centrifugal fan dimensions. [14]

The complete fan model (inlet duct, impeller, volute and outlet duct) is constructed in SPACE-CLAIM program as shown in fig. 3. In order to capture the flow filed in the fully developed region, a suitable length for the (inlet and outlet) duct must be given in order to properly achieve the uniform velocity profile. In the present validation the length of the inlet and outlet duct are five times the duct diameter. The rear distance in fig.2, between the hub and volute wall, is assumed to be 31.5 mm.

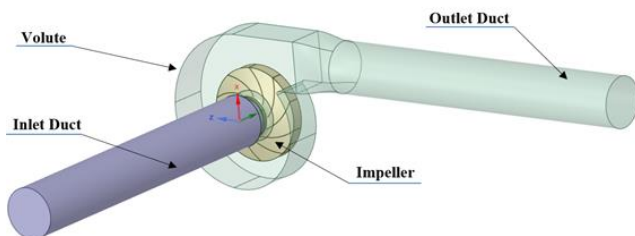


Fig 3. Complete 3D model created in Space-claim program, present validation.

3.2 Mesh Generation

The present computational solution utilizes a polyhedral mesh, where each individual cell has many neighbors and gradients can be approximated much more accurately than with tetrahedral. Additionally, polyhedral structures are less sensitive to stretching than tetrahedral structures, resulting

in greater numerical model stability [15]. Figure 4 shows the mesh used for inlet pipe (A) , impeller (B) and volute casing(C) using polyhedral elements.The leakage flow through the clearance between the impeller and inlet pipe (fig 4, D) has a great impact on the performance of the centrifugal fan. consequently, in the present validation, the gap dimensions mentioned in Table.1 is considered in present CFD simulations.

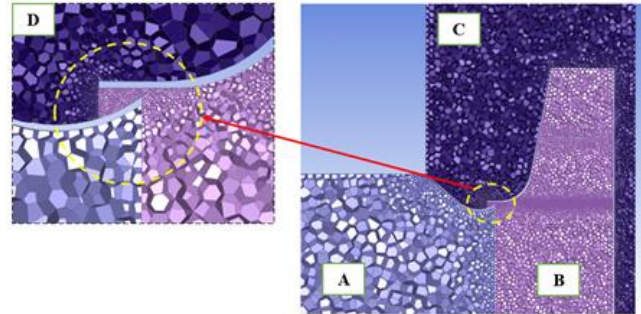


Fig 4. Polyhedral mesh at mid-section by FLUENT mesher program for: [A] Inlet pipe, [B] Impeller, [C] Volute and [D] A close view to the Impeller Volute

3.3 BOUNDARY CONDITIONS AND SOLUTION CONTROLS

The centrifugal fan's boundary condition consists of a velocity inlet boundary condition applied at the pipe inlet with a hydraulic diameter of 0.4 meters and a turbulence intensity of 5% in all tested fan performance points. The outflow boundary condition is used at the volute outlet. The hub, shroud, and fan blades are described as moving walls that revolve at zero velocity relative to the neighboring cell zone. The inlet pipe and volute casing are similarly defined as moving walls, but with zero absolute velocity. The impeller fluid domain is defined as frozen rotor (MRF) at 1500 RPM at the first numerical simulation with a fixed position relative to the volute casing, then the sliding mesh is applied to the impeller fluid domain for the unsteady simulation afterwards.

The solution is obtained by using SIMPLE algorithm between the pressure and velocity, three dimensions in space and steady in time (frozen rotor) for the first 2000 iterations, after that the mesh motion is applied to the unsteady calculations for one complete revolution and the flow statistics are initialized at the end. The iterations are then carried out again by rotating the impeller for a second revolution. During the second round, the data sampling for each time step is used to get a picture of how the flow changes over time.

3.4 CONVERGENCE HISTORY

The solutions for the centrifugal fan are obtained with this criterion. During the solutions, iteration history is also checked for the stability and the trend of the residual curves. Figure 5 shows a typical convergence history graphs for the steady and unsteady solutions obtained for the centrifugal fan. In Fig 5.A It is seen that for almost the first 2000 iterations the residuals for the variables are decreased to at least three orders of magnitude for steady solution. From 2000 to 5500 iterations the unsteady convergence shows a stable trend till the end. In Fig 5. (B, C and D) the

convergence histories of other solution variables like pressure outlet, pressure inlet and coefficient of moment (Cm) are also monitored to decide whether a reasonable solution is reached or not. unsteady graphs are divided into three convergence stages; each stage represents a complete revolution of the impeller. Stage 1 shows the transition from the steady to the unsteady calculations represented in dramatically change in the output value followed by some fluctuation to flow time at 0.04 seconds. Prior to the second stage, the flow statistic is initialized and calculations are done for the second impeller revolution to time 0.08 seconds. The final stage from 0.08 to 0.12 is carried out to insure that the output variables are unchanged.

3.5 MESH SENSITIVITY STUDY

Mesh size is one of the most influential elements in the outcomes of numerical simulations. To explore the flow

field across the critical areas of the centrifugal fan, it is necessary to construct the smallest elements around the blades, such as the leading and trailing edges, etc. In this section a mesh convergence test is carried out to assure that the CFD validation results is in a good agreement with the experimental results by Schönwald et al. [14]. In the present work, we used six different points starting from the coarse mesh (point 1) to the fine mesh (point 6). Figure 6 shows the effect of the number of cells on the Static pressure rise between the inlet and outlet of the fan (fig.6 A) and impeller torque (fig.6 B) for one of the cases of the validation study at flow coefficient of 0.027. The figures show that the results are almost independent of mesh elements number for all values of number of elements equal or above 3.4 million.

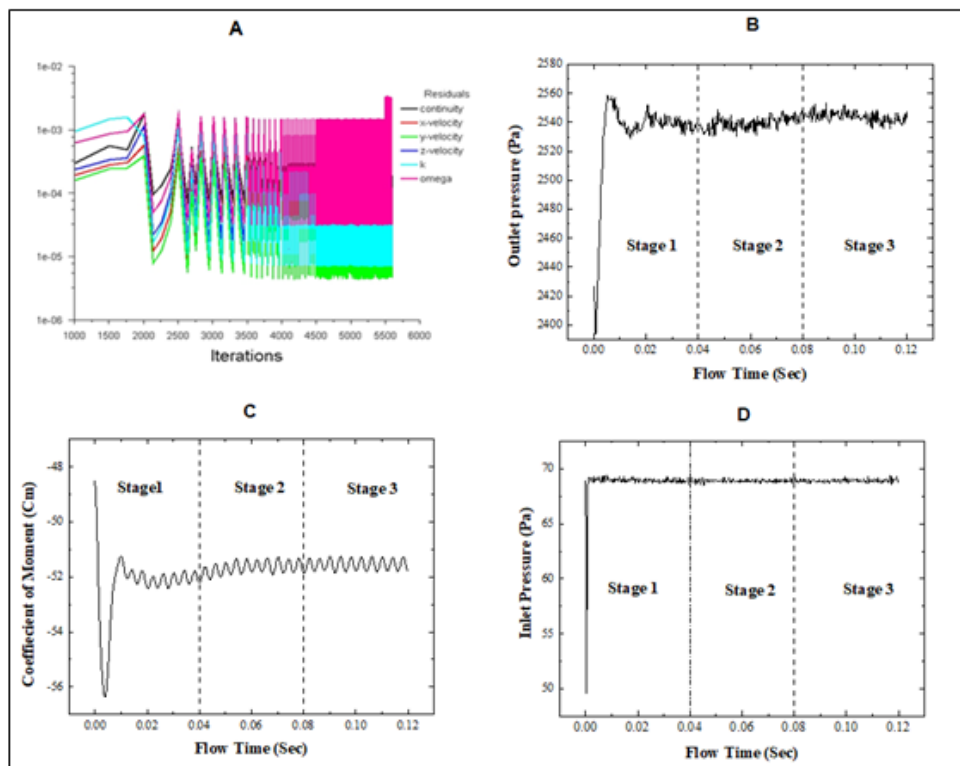


Fig 4. Convergence history graphs at [N=1500 RPM and $\Phi = 0.027$]: (A) Residuals graph for mass flow rate, velocity components, turbulence kinetic energy (K) and dissipation rate (ω), (B) outlet pressure, (C) Coefficient of moment CM and (D) Inlet pressure

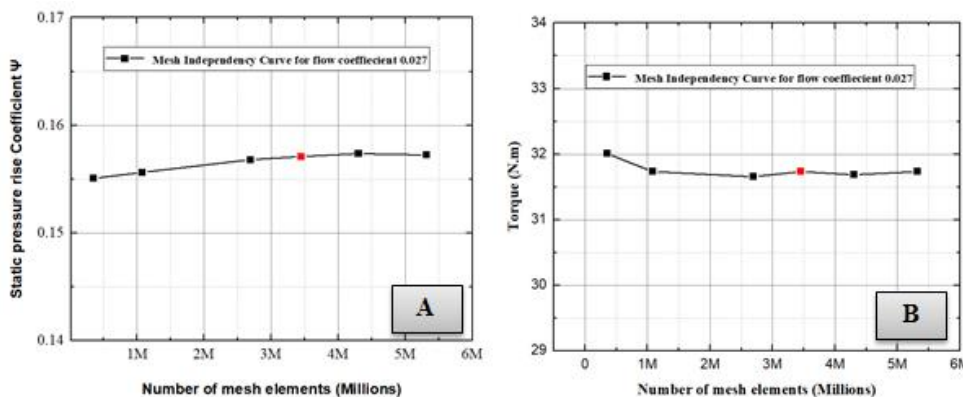


Fig 5. Effect of mesh elements number on the static pressure rise coefficient (A) and impeller torque (B) at flow coefficient 0.027

4. CFD VALIDATIONS RESULTS

The iterations for the performance points are made by assigning different inlet velocity values at the inlet pipe boundary of the domain, resulting in corresponding flow rates for the pressure differentials across the fan. The outlet boundary is outflow for all performance points. At the end the overall solution the performance curves for the centrifugal fan are given. Comparisons of the pressure contours and velocity distributions are presented and discussed.

4.1 Performance Curves Comparisons

The aerodynamic performance of the designed fan by Schönwald et al.[14] is simulated for the design rotational speed 1500 rpm. Present results are compared with their experimental measurement. comparisons of the experimental results of Schönwald et al with the present computational results are shown in fig. 7. Figure. 7 (A) shows the variation of the static pressure rise coefficient and the flow coefficient for the centrifugal fan. The unsteady pressure coefficient agrees well with the experimental results of Schönwald et al. across the entire flow coefficient range. The unsteady pressure curve gives more accurate values than those given by the steady calculations. This result came from the solution method of the unsteady simulation; the static pressure rise is measured under unsteady statistics by calculating the mean static pressure rise at each time step by rotating the impeller (3°) with 120 time steps during a complete rotation of the impeller. However, the steady pressure curve could be considered an initial guess for the fan pressure curve when computational time is limited.

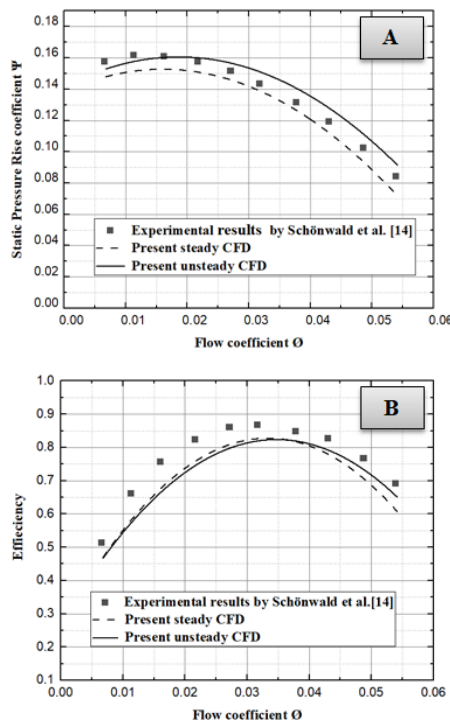


Fig 7. Comparisons between present results and experimental results of Schönwald et al. [14] at (N=1500 RPM): static pressure rise curved (Fig.A) and efficiency curves (Fig.B)

By comparing the efficiency curves in Fig.7 (B), the steady and unsteady curves have the same trend along the total flow coefficient values as the experimental results by Schönwald et al [14]. It is clear from the graph that both the steady and unsteady efficiency curves are still below the experimental curve by Schönwald et al. However, the unsteady efficiency curve shows good agreement with the experimental curve by Schönwald et al. among the steady calculations after flow coefficient 0.0321, with a difference in efficiency with the experimental of less than 3.5% for $\Phi= 0.032$ to the end of the curve, which is accepted. At low flow coefficients, the steady calculations show good agreement with the unsteady calculations from flow coefficient 0.0067 to the maximum efficiency point at flow coefficient 0. 0321.Finally, the comparisons serve as good verification of the used program, and it is possible to predict flow fields using the present CFD model.

4.2 CFD Post Processing Validation

Flow visualization is required to create a surface at the mid-section of the impeller to capture the flow separation inside the blade passages. Figures 8 [a] and [b] show a comparison of the streamlines colored by the magnitude of the velocity between Schönwald et al. and the present unsteady CFD on a plane at the mid-section of the impeller at the maximum efficiency point. Both graphs show that the flow separation occurs first after the midpoint of the blade in all impeller passages, and they show good general agreement between them.

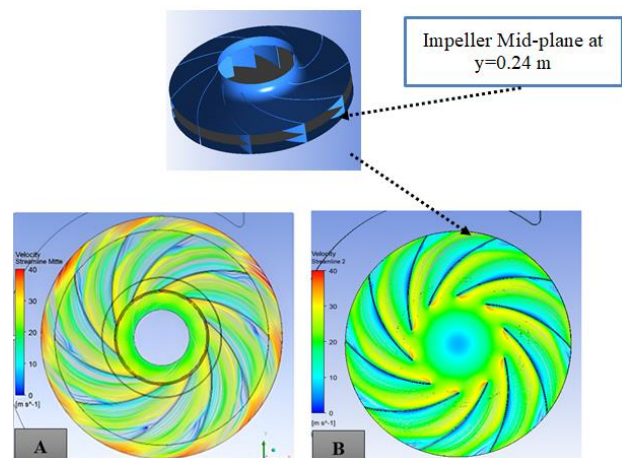


Fig 8. Velocity vectors and contours at a cross section in the centrifugal fan domain, [a] CFD by [14] and [b] CFD –present model

5. THE EFFECT OF THE SLOT’S LOCATION

A cut slot perpendicular on the blade span from the hub to the shroud with a constant width as shown in fig.10 is investigated numerically using the present validation model at various six configurations at diametric position ratios (DS/D) equal to 0.5, 0.6, 0.65, 0.7, 0.8, and 0.9, where (D) is the impeller diameter and (Ds) is the mean diameter at the cut slot, at a rotational speed of 1500 RPM, and with the other parameters remaining constant. Table 3 shows the parameters used to construct the six cases at different slot locations.

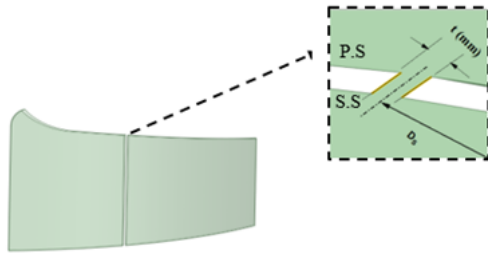


Fig 10. Slotted blade specifications in present work

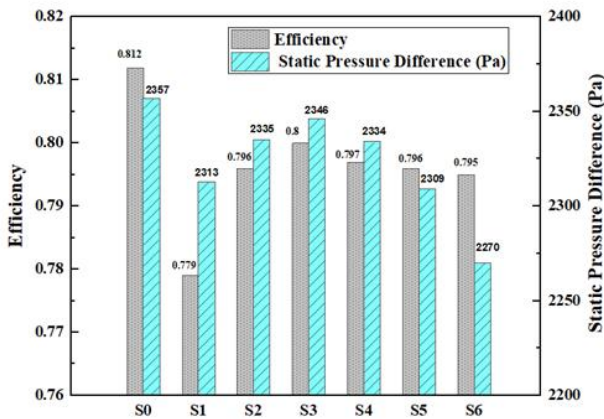


Fig 11. The effect of the slot locations on the fan efficiency and the fan static pressure rise at flow coefficient 0.0321

Figure 11. demonstrates the effect of changing the slot location along the blade span on the efficiency and the static pressure difference of a backward centrifugal fan at the BEP (best efficiency point) at flow coefficient 0.0321. The slot is shown to reduce the pressure rise and fan efficiency while it is known to reduce fan noise and pulsation outflows [6]. The figure shows that the location

of the blade slot has a considerable effect on the fan performance. The pressure decreased dramatically with configurations S1 and S6 near the leading and trailing edges, however the cut slot after the mid span of the blade increased the pressure. Slot located at D_s/D of 0.65 namely S3 gives the best performance compared with all tested locations.

Figure 12 and 13 display the streamlines colored by the velocity magnitude for the datum blade (S0) and slotted blades at different slot locations S1, S2, S3, S4, S5 and S6. For the datum blade, the streamlines at the suction side separated in all impeller passages. The point of separation appeared at one-third of the blade span from the blade's trailing edge. For the slotted blades in case S1 (near the leading edge), S5 and S6 (near the trailing edge), it is clear that an early separation occurs near the trailing edge of the blades compared with S0, these slot locations have a negative effect on the flow attachment near the blade surface. For cases S2, S3 and S4, have a general qualitative effect on the flow separation, these configurations showed that the separated flow is forced to the blade tip.

6. THE EFFECT OF THE SLOT'S WIDTH

In the following section, the effect of the slot width on the static pressure rise and fan efficiency was tested using four slot widths of 1.5 mm, 2.5mm, 3.5 mm, and 5 mm while keeping the best slot location S3 at (D_s/D of 0.65) as shown in fig. 14. Numerical simulation methods and same boundary conditions were applied to compare the unsteady performance, which includes the static pressure difference, efficiency, and internal flow field distribution.

TABLE.3 Slot's specifications.

Configurations	S ₀	S ₁	S ₂	S ₃	S ₄	S ₅	S ₆
Ds/D _{impeller}	-	0.5	0.6	0.65	0.7	0.8	0.9
D _s	-	361	433.2	469.8	505.4	577.6	649.8
Width	-	2.5	2.5	2.5	2.5	2.5	2.5

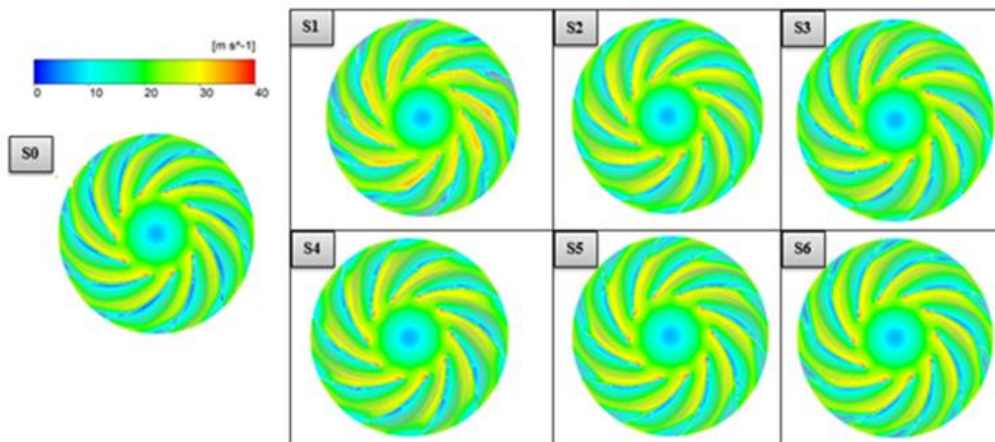


Fig 12. Streamlines comparisons colored by velocity magnitudes at flow coefficient 0.0321 between Datum Blades (S0) and slotted blades at six different locations

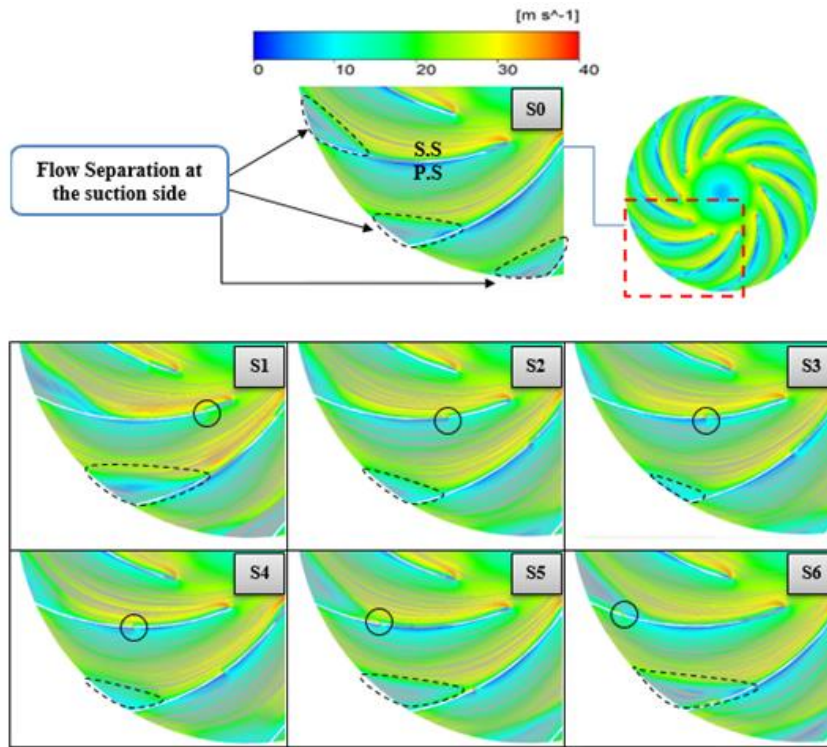


Fig 13. A close view of velocity streamlines comparisons in the blade passages at flow coefficient 0.0321 between the datum blade (S0) and slotted blades at six different locations

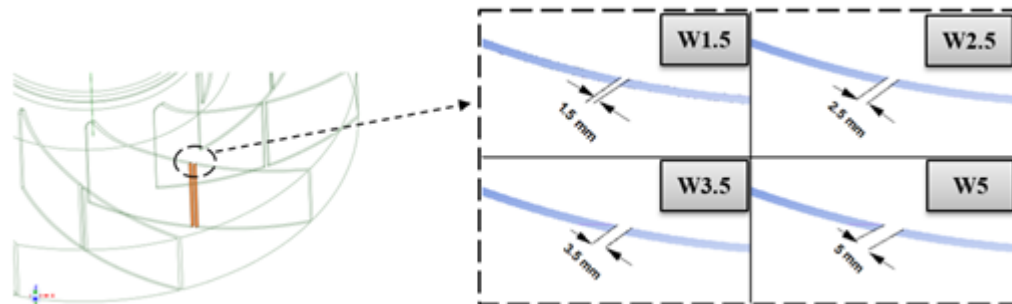


Fig 14. Fan blades with slot configuration S3 and different slot widths

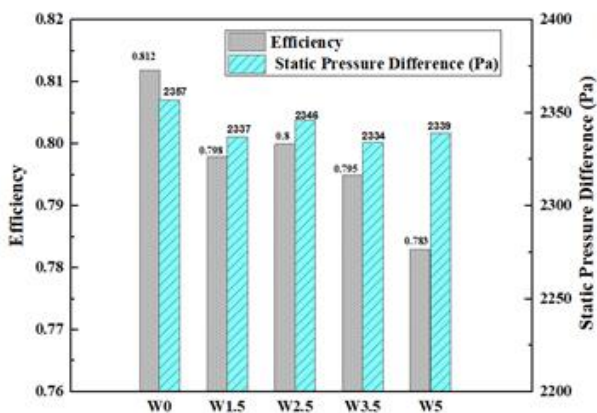


Fig 15. The effect of the slot widths on the fan efficiency and the fan static pressure rise at BEP (flow coefficient 0.0321) at location $D_s/D_{impeller}$ of 0.65

Figure 15 represents the effect of slot width on static pressure and efficiency at the BEP (flow coefficient of 0.0321). It is clear from the figure, that the slot configuration W2.5 corresponding to the location D_s/D of 0.65 and 2.5 mm width found to be the optimum configuration compared with the other ones (W1.5,3.5,5) and lower than the base model W0 (without slot) by 1% in efficiency. Additionally, as the slot width increase above than 2.5 mm, the fan efficiency and static pressure decreased. slot configuration W5 reduced the efficiency by 3% compared with the model W0.

Figure 16 illustrates the flow behavior near the suction side at different slot widths. The magnitude of the velocity of the jet of fluid coming out of the slot decreased as the slot width increased from 1.5 to 5 mm, resulting in a reduction in fluid momentum at the suction side. At Configuration W5, the boundary layer thickness increased, the reversed flow appeared and increased the

loss at the blade tip. Configuration w1.5 also increased the flow separation at the blade tip compared with the base model. On the other hand, models W2.5 and W3.5 streamlined the fluid over the blade surface and reduced the loss at the impeller outlet.

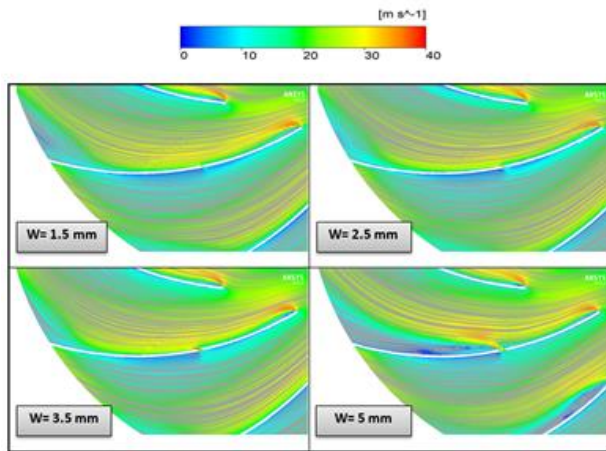


Fig 16. A close view of velocity streamlines comparisons in the blade passages at BEP between the confirmation (S3) and slotted blades with Different widths at the same location

7. Conclusions

The present study numerically investigated the effect of the location and width of a single cut slot in the impeller blades on flow behavior inside the blade passages and the fan performance. The results are concluded as the following:

- slot cut near the mid-span of the blade at (configurations S2, S3 and S4), the jet of fluid efflux from the pressure side to the suction side through the slot increased the fluid velocity and forced the recirculated flow toward the blade tip and let the boundary layer build up over the blade suction side. S3 is considered as the best location among all the tested locations. conversely, slots cut near the blade leading edge (configuration S1) and near the trailing edge (configuration S5 and S6) boosted the boundary layer separation over the blade and resulting an early separation compared with the base model S0 (without slots).
- Increased the slot width up to 5 mm reduced the fluid momentum at the slot outlet and the efficiency dropped by 2% compared with configuration S3.
- The optimum slot configuration for the used impeller is S3 with 2.5 mm width and at location at D_s equal to 0.65 of the impeller diameter and at 37 % of the span from the blade leading edge.
- Slot cut in the impeller blades from the hub to the shroud at any location decreased the efficiency and pressure rise coefficient across compared with the base model S0 while slotted blades are known to reduce noise and pulsating outlet flow [6].

REFERENCES

- [1] Schlichting, "Boundary Layer Theory," Seventh Ed. McCraw-Hill, 1968.
- [2] T. L. Le, T. T. Nghia, H. D. Thong, and M. H. K. Son, "Numerical Study of Aerodynamic Performance and Flow Characteristics of a Centrifugal Blower," *Int. J. Intell. Unmanned Syst.*, 2022, doi: 10.1108/IJIUS-07-2021-0076/FULL/PDF.
- [3] Y. Li, D. H. Rowinski, K. Bansal, and K. R. Reddy, "CFD Modeling and Performance Evaluation of a Centrifugal Fan Using a Cut-Cell Method With Automatic Mesh Generation and Adaptive Mesh Refinement," in 24th International Compressor Engineering Conference at Purdue, Jan. 2018. [Online]. Available: <https://docs.lib.purdue.edu/icec/2622>
- [4] H. Ding, T. Chang, and F. Lin, "The influence of the blade outlet angle on the flow field and pressure pulsation in a centrifugal fan," *Processes*, vol. 8, no. 11, pp. 1–14, 2020, doi: 10.3390/pr8111422.
- [5] M. S. Kassim, F. A. Saleh, and M. A. Kadhun, "Experimental and Numerical Investigation of Blades Slots on Rotating Stall Phenomenon in Centrifugal Blower," *Univers. J. Eng. Sci.*, vol. 3, no. 2, pp. 24–37, May 2015, doi: 10.13189/UJES.2015.030203.
- [6] A. Pieruszka, T. Siwek, W. Kalawa, Ł. Lis, S. Stefański, and K. Sztokler, "The Effect of Blade Slots on Flow Behaviour in a Fan Impeller," *EPJ Web Conf.*, vol. 02067, pp. 1–4, 2019, doi: 10.1051/epjconf/201921302067.
- [7] H. G. Zhang, F. Y. Dong, X. D. Zhang, and W. L. Chu, "Numerical Investigation of Effect of Blade Surface Slot on the Performance and Flow Field of a Low Speed Centrifugal Fan," *Proc. ASME Turbo Expo*, vol. 2E-2020, Jan. 2021, doi: 10.1115/GT2020-14472.
- [8] N. Madhwesh and K. V. Karanth, "Effects of Innovative Suction Slots on the Performance of a Radial Bladed Impeller of a Centrifugal Blower - A Numerical Transient Analysis," *espublisher*, vol. 17, pp. 91–100, Dec. 2021, doi: 10.30919/ES8D587.
- [9] R. Rong, K. Cui, Z. Li, and Z. Wu, "Numerical Study of Centrifugal Fan with Slots in Blade Surface," *Procedia Eng.*, vol. 126, pp. 588–591, Jan. 2015, doi: 10.1016/J.PROENG.2015.11.309.
- [10] Y. Xie, J. Chen, H. Qu, G. Xie, D. Zhang, and M. Moshfeghi, "Numerical and experimental investigation on the flow separation control of S809 airfoil with slot," *Math. Probl. Eng.*, vol. 2013, doi: 10.1155/2013/301748.
- [11] Q. Ke and L. Tang, "Performance Optimization of Slotted Blades for Low-Specific Speed Centrifugal Pumps," *Adv. Civ. Eng.*, vol. 2023, doi: 10.1155/2023/9612947.
- [12] H. K. Versteeg and W. Malalasekera, *An Introduction to Computational Fluid Dynamics: The Finite Volume Method*, vol. Second Ed. 1996.
- [13] F. R. Menter, "Zonal Two Equation $k-\omega$ Turbulence Models for Aerodynamic Flows," *AIAA 23rd Fluid Dyn. Plasmadynamics, Lasers Conf.*, 1993, doi: 10.2514/6.1993-2906.
- [14] S. Schönwald, F. Kameier, and M. Böhle, "Influence of the Casing Width and the Impeller Position on Centrifugal Fan Performance - A CFD-Based Study on Cause and Effect," *Proc. ASME Turbo Expo*, vol. 1A, 2014, doi: 10.1115/GT2014-25319.
- [15] M. Sosnowski, J. Krzywanski, and R. Gnatowska, "Polyhedral Meshing as an Innovative Approach to Computational Domain Discretization of a Cyclone in a Fluidized Bed CLC Unit," *Energy and Fuels*, vol. 14, p. 1027, Jan. 2017, doi: 10.1051/e3sconf/20171401027.